Nuclear Instruments and Methods in Physics Research B 268 (2010) 1277–1282

Contents lists available at ScienceDirect

Nuclear Instruments and Methods in Physics Research B

journal homepage: www.elsevier.com/locate/nimb

Nuclear astrophysics and AMS – Probing nucleosynthesis in the lab

Anton Wallner *

Vienna Environmental Research Accelerator (VERA) Laboratory, Faculty of Physics, University of Vienna, Währinger Str. 17, 1090 Wien, Austria

A R T I C L E I N F O

Article history:
Available online 7 October 2009

Keywords:
Nucleosynthesis
Activation
AMS
Long-lived radionuclides
Cross-section
$^{9}Be(n,\gamma)^{10}Be$
$^{13}C(n,\gamma)^{14}C$
$^{54}Fe(n,\gamma)^{55}Fe$

A B S T R A C T

Nuclear astrophysics aims at describing nuclear processes relevant to nucleosynthesis. Such reactions can be studied by performing nuclear cross-section measurements at the relevant energy regimes. Accelerator-based experiments allow simulating nucleosynthesis in the laboratory. For specific reactions accelerator mass spectrometry (AMS) offers a powerful tool to measure cross-sections independent on half-lives of reaction products. It represents a complementary, off-line method compared to on-line methods, the latter being sensitive to prompt reaction signatures. An overview over recent experiments using AMS in nuclear astrophysics is given and for selected reactions the potential of AMS is exemplified: limitations and advantages of this method are illustrated for neutron-induced reactions on ^{9}Be, ^{13}C and ^{54}Fe, leading to the long-lived AMS isotopes ^{10}Be, ^{14}C, and ^{55}Fe, respectively. Measurements on ^{55}Fe allow producing highly precise data. The potential of AMS for helping to resolve a recently observed discrepancy between observation and nucleosynthesis models relevant for our understanding of the isotopic abundances is highlighted.

1. Introduction

One of the ongoing questions in nuclear astrophysics is a better understanding of the elemental abundances of the solar system. While the very light elements from hydrogen to lithium are found to be dominantly produced in the early phase after the Big Bang, elements from carbon to the heaviest ones are understood to be synthesized in nucleosynthesis processes in stars: the isotopic pattern of our solar system [1] which is strongly mirrored in extra-solar objects is a fingerprint of stellar nucleosynthesis processes within many generations of stars. The complex isotopic signature can be understood as the interplay of nuclear physics issues and the specific conditions of the stellar environment [2]. Charged-particle induced reactions are responsible for the production of the nuclides from carbon up to Fe and Ni, while most of the elements heavier than iron are produced via neutron-induced reactions. Finally, specific processes, e.g. *p* and *rp*-process, help to tailor the isotopic abundance pattern for some proton-rich nuclei across the chart of nuclides [3].

Element synthesis of the lighter masses is dominated by charged-particle induced reactions during the stellar burning phases. Relevant are often a few resonances within a narrow energy range. Typical particle energies range from tens of keV up to several MeV. In a few cases, longer-lived radionuclides like ^{26}Al and ^{44}Ti, can be traced in the sky via observing their characteristic decay pattern, e.g. by space-born γ-ray telescopes. Their intensity distribution represents an important source of information to identify active nucleosynthesis regions in our galaxy. In this regard, AMS has been used to measure such production rates, e.g. of ^{44}Ti dominated by the $^{40}Ca(\alpha, \gamma)$ reaction [4], and of ^{26}Al through the $^{25}Mg(p, \gamma)$ reaction [5].

Neutron-induced reactions are triggered by two different scenarios [2]: the slow neutron-capture process (*s*-process) and the rapid neutron-capture process (*r*-process) – both contribute about equal to the abundance of elements above iron. They are characterized by the time scale of the reaction rate relative to their competing beta decays. The *s*-process acts at time scales of months to years, it can be subdivided into tree fractions, corresponding to different mass regions, temperature ranges and neutron exposures [6,7] in late phases of stellar burning. In particular for *s*-process calculations in the lower-mass range ($A < 90$), uncertainties are still large because the corresponding neutron-capture cross-sections are not sufficiently well known. Accuracy of the order of 3% would be necessary for proper calculations [8]. Interestingly, recent observations of very old, so-called ultra-metal-poor (UMP) stars indicate that our knowledge of heavy-element nucleosynthesis is still limited [9]. New precise measurements might help to clarify this recently found discrepancy in UMP stars (see Section 4).

r-process nuclides need high neutron densities, most likely provided in supernova (SN) explosions, possibly, but less likely, in merging neutron stars. Supernova (SN)-produced, long-lived

* Address: VERA Laboratory, Fakultät für Physik – Isotopenforschung, Universität Wien, Währinger Straße 17, A-1090 Wien, Austria. Tel.: +43 1 4277 51711; fax: +43 1 4277 9517.
E-mail address: anton.wallner@univie.ac.at

0168-583X/$ - see front matter
doi:10.1016/j.nimb.2009.10.152

radionuclides deposited on Earth [10–12], like ^{60}Fe, ^{182}Hf, ^{244}Pu and ^{247}Cm (see e.g. [13–19]), and possibly super-heavy elements [20], will give an improved insight into explosive nucleosynthesis scenarios. AMS represents a powerful and sensitive technique to search for live long-lived radionuclides in terrestrial archives, as signatures of both, single close-by SN explosions and steady-state (i.e. averaged) concentrations of such nuclides [21].

There is a clear need for more data to support our understanding of these processes. One important contribution to the study of nuclear processes occurring in stars can be provided by measurements of nuclear reactions at accelerator based facilities. AMS offers a powerful tool to measure cross-sections independent on half-lives of reaction products. In Section 2 a summary of AMS contributions to cross-section measurements of relevance in nuclear astrophysics is given: charged-particle and neutron-induced reactions are listed. In the subsequent sections, for a few specific cases of neutron-capture reactions, some AMS-relevant features are presented. Those cases demonstrate that also standard applications of AMS will benefit from such "exotic" measurements, where the facility has to explore its detection limits.

2. Cross-section measurements in nuclear astrophysics using AMS

AMS contributed to understand and validate nucleosynthesis through various cross-section measurements. Activation with subsequent AMS measurements have been applied for isotopes where off-line decay counting is difficult or impossible due to long half-lives or due to the absence of suitable γ-ray transitions. Paul and co-workers first introduced AMS to cross-section measurements in nuclear astrophysics for the ^{26}Mg(p, n)^{26}Al reaction [22] and later for neutron-induced reactions [23] using a stellar-like neutron spectrum developed at FZK (for more details see Section 3 and Ref. [24]). AMS measurements in combination with charged-particle induced reactions have been proposed first for the measurement of ^{40}Ca(α, γ)^{44}Ti [25,4] and also for ^{25}Mg(p, γ)^{26}Al [26,5]. A list of AMS measurements studying reactions of interest for stellar processes is given in Table 1.

3. Neutron-capture cross-section measurements at VERA

In the following, advantages and limitations of AMS measurements are illustrated for neutron-induced reactions. Their typical stellar environments correspond to particle energies in the range of keV. In particular, *s*-process nucleosynthesis knows two dominating phases [6–8]: the *main* component takes place at kT = 8 keV (important for element production between A = 90 and 204). The second, *weak* component (at somewhat higher energies, kT = 25 keV), contributes dominantly to element production between the seed nuclei, Fe and Ni, and up to A = 90.

Neutron activations in combination with AMS were usually performed at Forschungszentrum Karlsruhe (FZK) [24]. Neutrons were produced via the ^{7}Li(p, n)^{7}Be reaction. By choosing a proper irradiation geometry, a quasi-stellar neutron spectrum is generated which approximates a Maxwellian distribution for kT = 25 keV [24]; increased proton energies allow also to produce higher neutron energies. Such an irradiation covers simultaneously the energy region of interest. Depending on the cross-section value, isotope ratios between 10^{-11} and 10^{-14} were produced at FZK. After the neutron irradiation, the subsequent AMS measurements were performed at the various AMS facilities, like Argonne, Munich or Vienna (see Section 2). In the following, a few specific reactions measured at the Vienna Environmental Research Accelerator (VERA) are highlighted with respect to interesting features for AMS measurements.

3.1. ^{9}Be(n, γ)^{10}Be neutron-capture cross-section measurement

Low-mass nuclei like ^{9}Be or ^{13}C exhibit low neutron-capture cross-section values. Therefore, to be of relevance for nucleosynthesis, high neutron densities are needed, as proposed, e.g. in inhomogeneous Big-Bang nucleosynthesis scenarios or in explosive nucleosynthesis, like short time-scale *r*-process [42,43]. In all those cases, the high neutron densities allow to overcome the obstacle of unstable masses at A = 5 and A = 8, which otherwise stops nucleosynthesis above the seed nucleus ^{4}He almost completely. However, up to date, no experimental values can be found for ^{9}Be(n, γ)^{10}Be neutron capture above thermal energies. Adopted values for keV energies are extrapolations from the only existing thermal values and they scatter by more than a factor of 10 [32].

Samples of commercially available BeO powder were irradiated at FZK with neutrons corresponding to a Maxwellian–Boltzmann distribution of kT = 25 keV, and with energies of 500 keV. The number of ^{10}Be nuclei produced during the neutron irradiations, scales directly with the neutron flux (neutrons cm^{-2} and s^{-1}), the neutron-capture cross-section value and the duration of the neutron irradiation. A neutron flux of (1–2) $\times$ 10^{9} neutrons cm^{-2} s^{-1} corresponds to a total of (0.6–1.2) $\times$ 10^{15} neutrons cm^{-2} within a reasonable irradiation period of 1 week. According to semi-empirical studies, a cross-section value between 1 and 100 μbarn is expected for ^{9}Be(n, γ)^{10}Be at 25 keV. Combining all these values results in an expected isotope ratio ^{10}Be/^{9}Be between 6×10^{-16} and 1.2×10^{-13}.

Commercially available BeO samples typically contain ^{10}Be at concentrations comparable to that expected from the neutron irradiation. In general, for cases where signal and background are of the same order, a stable and well-defined background signal has to be fulfilled.

For ^{9}Be(n, γ)^{10}Be, different BeO pellets were available from independent neutron irradiations. Fig. 1 shows the ^{10}Be/^{9}Be isotope ratios measured for two BeO samples. Be-sample no. 1 (upper figure) was exposed to a lower neutron fluence compared to sample no. 2 (lower one). This is reflected in different individual ^{10}Be/^{9}Be ratios (symbols). Lines depict the mean values for the irradiated samples and unirradiated blanks. Dashed lines indicate the uncertainty associated with the mean values. In order to highlight contributions from systematic uncertainties, in the upper panel statistical errors are given only, while the lower one includes systematic uncertainties, too. Combining the background-corrected isotope ratios of the two samples with their corresponding neutron fluence, results in a cross-section value (averaged for 25 keV) of (9.2 ± 0.5) and (9.8 ± 0.8) μbarn, respectively, in good agreement to each other.

Recently, an additional neutron irradiation was performed at an energy of 500 keV. A resonance might occur at that energy, but, because of a significantly lower neutron yield in the irradiation, the isotope ratio is expected to be even lower than that for 25 keV. Interestingly, the growing interest for geological applications in a Be spike material with lowest ^{10}Be content, led to the finding of Be-containing materials with isotope ratios well below 10^{-14}. At VERA such material was measured to ^{10}Be/^{9}Be ratios of <10^{-15} [44]. Such a material was utilized for measuring the cross-section at 500 keV.

Within these measurements the VERA facility could demonstrate both, a low machine background without ^{10}B and ^{9}Be interference [45], and good measurement reproducibility. The reference material used for ^{10}Be measurements (Zurich S555, with a quoted isotope ratio of 9.55×10^{-11}), however, gave rise to a source cross contamination of about 10^{-14}. This effect was below the detection limit in previous applications. For measurements with ratios of 10^{-14} or below, such a cross contamination has to be avoided. To this end, BeO powder material was activated with thermal neu-

Table 1
Some cross-section measurements of interest to nuclear astrophysics using AMS. Neutron activation in combination with AMS was almost exclusively done at FZK [24]. New measurements are also proposed at Notre Dame, e.g. ^{78}Kr(α, γ)^{82}Se. FZK: Forschungszentrum Karlsruhe and FZD: Forschungszentrum Dresden-Rossendorf.

Reaction	Projectile	Irradiation facility	Particle energy	AMS facility	References
^{26}Mg(p, n)^{26}Al	p	Argonne FN tandem	5.3–7.0 MeV	Argonne tandem	[22]
^{25}Mg(p, γ)^{26}Al	p	FZD, implanter	189–418 keV	Munich/Vienna	[5,26]
^{25}Mg(p, γ)^{26}Al	p	LUNA, Gran Sasso	189–304 keV	CIRCE Caserta	[27], in progress
^{40}Ca(α, γ)^{44}Ti	^{40}Ca	ATLAS (Argonne)	~ 4.2 MeV resonances	Hebrew Univ./Weizmann Inst.	[4,25,28,29]; inv. kinematics
^{40}Ca(α, γ)^{44}Ti	^{40}Ca	Koffler tandem, Weizmann Inst.	2.1–4.2 MeV integral	Hebrew Univ./Weizmann Inst.	[4,29] inv. kinematics
^{40}Ca(α, γ)^{44}Ti	^{40}Ca	Munich MP tandem	2.1–4.17 MeV and 4.17–5.39 MeV (integral)	Munich – GAMS	[30], in progress, inv. kinematics
^{62}Ni(n, γ)^{63}Ni	n	FZK	25 keV	Argonne – ATLAS	[23,31]
^{9}Be(n, γ)^{10}Be	n	FZK	25 keV, 500 keV	Vienna – VERA	[32], in progress
^{13}C(n, γ)^{14}C	n	FZK	25 keV, 128 keV, 167 keV	Vienna – VERA	[32], in progress
^{14}N(n, p)^{14}C	n	FZK	25 keV, 123 keV, 178 keV	Vienna – VERA	in progress
^{40}Ca(n, γ)^{41}Ca	n	FZK	25 keV	Vienna – VERA	[33,34]
^{54}Fe(n, γ)^{55}Fe	n	FZK	25 keV, 500 keV	Vienna – VERA	[33,35], in progress
^{58}Ni(n, γ)^{59}Ni	n	FZK	25 keV	Munich – GAMS	[36]
^{62}Ni(n, γ)^{63}Ni	n	FZK	25 keV	Munich – GAMS	[37], also ^{64}Ni(γ,n)
^{78}Se(n, γ)^{79}Se	n	FZK	25 keV	Munich – GAMS	[36,37]
^{209}Bi(n, γ)^{210m}Bi	n	FZK	25 keV	Vienna – VERA	in progress
^{147}Sm(n, 2n)	n	Tohoku Univ.	n: 6–10 MeV	Argonne – ATLAS	[38,39], in progress
^{147}Sm (p, 2nε)	p	Osaka Univ.	p: 21 MeV		
^{147}Sm (γ, n)	γ	Tohoku Univ.	γ: ⩽50 MeV		
^{40}Ca(α, γ)^{44}Ti	^{40}Ca	Univ. Notre Dame	~4.2 MeV	U Notre Dame	[40], in progress
^{33}S(α, p)^{36}Cl, ^{36}S(p, n)^{36}Cl	^{36}S	Univ. Notre Dame	5–7 MeV	U Notre Dame	[41], in progress

trons in a reactor to produce reference materials with isotope ratios between 10^{-13} and 10^{-12}. Nevertheless, one always relies on the absolute value of the standard material used. In particular, for ^{10}Be measurements this is currently important, because of previously discrepant half-live values associated with standard materials. Thanks to new measurements, the half-live value of ^{10}Be now seems to converge to a value of (1.387 ± 0.012) Myr with high precision [46,47].

3.2. ^{13}C(n, γ)^{14}C neutron-capture cross-section measurement

Besides Big Bang and highly neutron-rich environments, this reaction is also of interest in stellar burning processes: ^{13}C is one major product in CNO hydrogen burning. In addition, the reaction ^{13}C(α, n)^{16}O is the most relevant neutron source for the main *s*-process. Interestingly, the reaction ^{13}C(n, γ)^{14}C acts as a neutron poison in two ways: neutron capture removes both, ^{13}C as target for the neutron-producing reaction, and it consumes also neutrons, which otherwise will be used in the *s*-process for capture reactions. In addition, ^{13}C(n, γ)^{14}C is of importance in so-called neutron-induced CNO cycles [48].

Similar to the case of ^{9}Be(n, γ)^{10}Be, cross-section values of the order of 10 μbarn are expected. However, natural carbon consists of only 1% of ^{13}C, therefore, even one week of neutron irradiation (1×10^{15} neutrons cm^{-2}) results in an isotope ratio of ^{14}C/^{13}C = 1×10^{-14}, which translates to a ^{14}C/^{12}C isotope ratio of 1×10^{-16}. Clearly, enriched material has to be used for that purpose. A suitable ^{13}C-enriched material, low in ^{14}C, was available (amorphous graphite powder, provided by AMT Ltd., Israel). It is enriched by a factor of ≈10^4 compared to natural graphite. Such high ^{13}C concentrations, however, resulted in an enhanced blank ^{14}C/^{12}C isotope ratio. The reason was a "leaky" ^{13}C-beam entering our standard particle detector used for ^{14}C-dating applications. These signals were indistinguishable from true ^{14}C events. That detector-setup is located after the high-energy magnet and a 90° electrostatic deflector (ESA). Narrow slits after the ESA allowed cutting the leaking ^{13}C-beam significantly, but at the cost of fluctuating isotope ratios, being highly sensitive to terminal-voltage fluctuations. However, other detectors (an ionization chamber – labelled detector 1 in Fig. 2, and a TOF-detection setup – detector 2) positioned after an additional magnetic deflector (see [33] for the VERA setup), gave stable isotope ratios ^{14}C/^{13}C = (9.5 ± 0.5) × 10^{-15} for unirradiated graphite (Fig. 2).

Because of the low ^{14}C content in the samples, one has to take care not to contaminate the enriched graphite material with natural carbon. It should be noted, that no chemistry was involved for those measurements – the irradiated material was directly pressed into sputter sample holders. Most of the samples showed ^{13}C/^{12}C values around 70; contamination with natural carbon would directly be reflected in a lower ^{13}C/^{12}C value.

A preliminary mean value for a sample irradiated with neutrons of *kT* = 25 keV (asterisk) is plotted in Fig. 3 and is compared to the two previous results [49,50], which were obtained from direct measurements (see also Section 4). The AMS value fits well to the previous data and all experimental values exclude the low values at 25 keV expected from theory [51]. As indicated in Fig. 3 two additional measurements at higher neutron energies are in progress. From theoretical investigations an increase in the cross-section value up to a factor of 1000 is possible for neutron energies at 150 keV (note the logarithmic scale in Fig. 3).

3.3. Other neutron-induced reactions measured at VERA

Besides the above mentioned reactions, several additional neutron-induced reactions of relevance to nuclear astrophysics are studied (see also [32,33]). The production of ^{14}C via ^{14}N(n, p) has been recognized as an important reaction in the CNO cycle. It represents the most important neutron poison in the late phases of stars and protons produced in that (n, p) reaction are essential in the – still not fully understood – nucleosynthesis of ^{19}F [52]. Samples containing both nitrogen and carbon (Uracil, $C_4H_4N_2O_2$) have been irradiated with neutrons with energies from thermal to MeV and are analyzed by AMS. An interesting case for comparing different experimental techniques is ^{54}Fe(n, γ)^{55}Fe: ^{55}Fe does not suffer from isobaric interferences and allows to generate precise AMS-data (see Section 4). At higher masses, the reaction ^{209}Bi(n, γ),

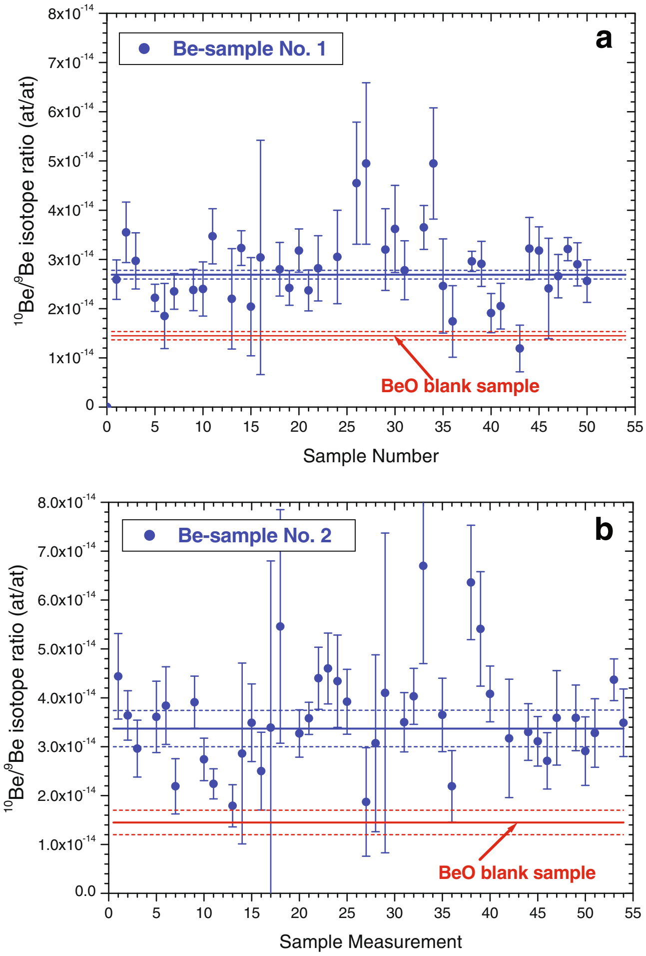

Fig. 1. ^{10}Be/^{9}Be isotope ratios from two independently irradiated BeO samples. Symbols depict the mean ratios of individual sputter samples. Solid and dashed lines indicate mean values and their uncertainties for irradiated samples and unirradiated controls. The value obtained for the blank (non-irradiated BeO) is the mean from various sputter targets (the individual data point are not shown for clarity of the display). Uncertainties given in the left panel include statistical uncertainties only; the right panel includes systematic contributions as well.

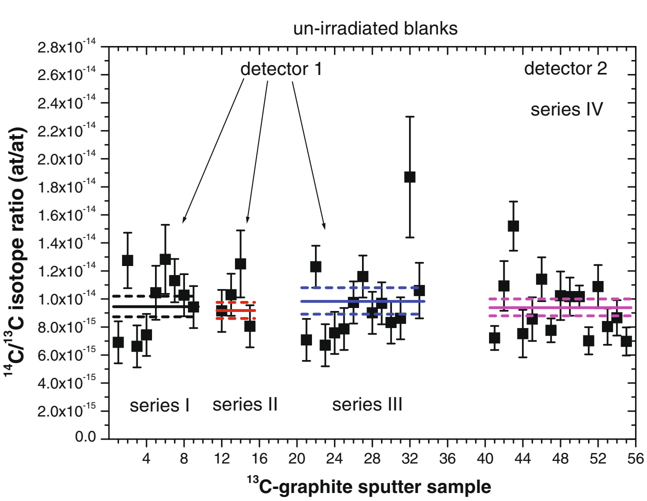

Fig. 2. Isotope ratios $^{14}C/^{13}C$ for highly enriched ^{13}C-graphite powder. The data were obtained with a particle detector where the beam had to pass a 90° high-energy magnet, a 90° electrostatic deflector and an additional magnetic switcher. The latter magnet sufficiently reduced interferences from a "leaky" ^{13}C-beam. Detector 1 and detector 2 represent an ionization chamber and the TOF-detection setup, respectively.

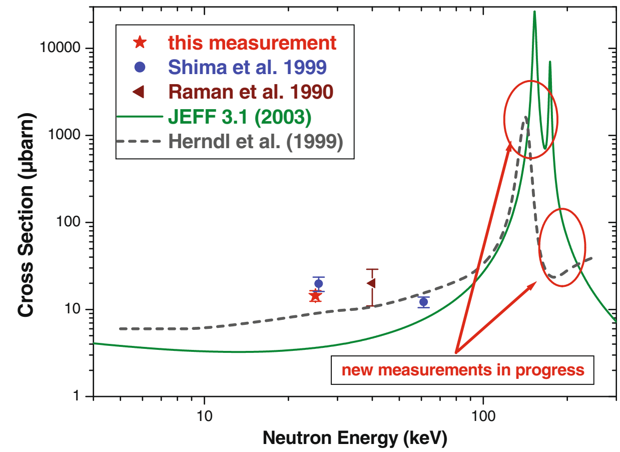

Fig. 3. $^{13}C(n,\gamma)^{14}C$ cross-sections in the neutron energy range of relevance for nuclear astrophysics scenarios (keV range). Two previous measurements (Shima et al. [49] and Raman et al. [50]) are in good agreement with the preliminary AMS value – in contrast to theoretical descriptions. Additional samples were irradiated and AMS measurements are in progress for a detailed investigation of the resonance region at higher neutron energies.

leading to the short-lived ^{210g}Bi ($t_{1/2} = 5$ days) and the long-lived isomer ^{210m}Bi ($t_{1/2} = 3.0$ Myr) is studied. That reaction terminates the *s*-process, because no stable or sufficiently long-lived nuclide can further be produced via slow neutron-capture processes. Although no stable isobar exists for ^{210}Bi, the decay product of ^{210g}Bi, ^{210}Po ($t_{1/2} = 138.4$ days), with its much higher negative ionization yield, interferes with ^{210m}Bi. The low cross-section value also requires suppressing efficiently interference from stable ^{209}Bi.

4. Comparison of AMS measurements to other techniques

Cross-section measurements can be classified into two complementary techniques: on-line and off-line methods. The on-line method makes use of the detection of the prompt and characteristic radiation associated with the production of a specific nuclide, or selectively detects the reaction product itself by means of the recoil separator technique (direct detection techniques). Typical examples of experimental facilities dedicated also to nuclear astrophysics studies in "direct mode" are, among many others, e.g. the DRAGON setup at TRIUMF (combined with recoil separator technique [53]), LUNA at Gran Sasso [54] and the Recoil Separator ERNA [55] for charged-particle induced reactions; and e.g. the n_TOF facility at CERN [56] for studying neutron-induced reactions. In addition, indirect detection techniques, e.g. the "Trojan Horse"-like methods and others (see [57]) are capable to investigate energy regions inaccessible to the direct techniques suffering from extremely low reaction rates.

A second and independent method in "off-line" mode makes use of the activation technique, with sample irradiation and subsequent measurement of the reaction product. After the irradiation the number of produced radioactive nuclei can be quantified either by decay counting or by mass spectrometric methods. This method is mostly restricted to radioactive products; however, it represents a very sensitive technique due to potential long irradiation periods. Stellar conditions can directly be simulated by generating a quasi-stellar spectrum (see e.g. [24]), and consequently the reaction rate directly scales with stellar rates. Contrary, direct methods have the advantage that, e.g. with the time-of-flight technique, an energy-dependent cross-section over a wide energy range can be obtained. Direct methods can be applied to both radioactive and stable reaction products, and can be applied to radioactive beams.

Nowadays, detection-setups are becoming state-of-the-art which offer higher detection efficiencies (e.g. in 4π geometry) compared to AMS [27].

The determination of the stellar cross-sections via the combination of the activation technique and AMS represents an important off-line method. It is complementary to on-line measurements, since this independent approach implies different systematic uncertainties. In this regard, precision measurements of neutron-capture cross-sections of ^{54}Fe are in progress to clarify the recently found discrepancy of *s*-process nucleosynthesis at lower-mass nuclei ($A < 120$). The discrepancy is related to observations of *r*-process elements in ultra metal-poor stars [9]. In such stars the abundance for elements heavier than barium scales exactly with the *r*-process abundances found in the solar system, while those lighter than barium show a systematic deviation of the order of 20%. A similar discrepancy is found for *s*-only isotopes lighter than barium (nuclides with no *r*-process contribution). These facts hint to some deficiency in the standard description of the *s*-process nucleosynthesis or there is a systematic offset in the experimental data. The latter can be tested by precision measurements of neutron-capture cross-sections, e.g. the ^{54}Fe(n, γ)^{55}Fe reaction.

The potential and power of AMS for detecting ^{55}Fe has been demonstrated recently in a first irradiation campaign [35]. ^{55}Fe detection benefits from the fact that no isobaric interference exists because ^{55}Mn does not form stable negative ions. At VERA AMS allows to perform measurements on the level of 1% reproducibility with a background level ^{55}Fe/^{56}Fe $< 2 \times 10^{-15}$ [33]. In this regard, an important aspect is the availability of accurate AMS standards. A new ^{55}Fe standard for AMS measurements is produced via the p-induced reactions ^{58}Ni(p, α) and ^{54}Fe(p, γ): in both cases ^{55}Co was produced, which decayed to ^{55}Fe with a half-life of 17.54 h. Combining the well-known half-life of ^{55}Co and the precisely measured activity of ^{55}Co allowed to calculate the amount of ^{55}Fe with high precision. In addition, a reference solution with a well-known concentration of ^{55}Fe is available; via a dilution series AMS reference material is produced. Measurements for ^{54}Fe(n, γ)^{55}Fe from thermal to several hundred keV neutron energies are now in progress at the VERA laboratory. The new data are expected to be accurate to a level of about 3%.

5. Conclusion

The actual situation of cross-section data relevant for nucleosynthesis is far from being satisfactory for a wide range of nuclides. The determination of the stellar cross-sections via a combination of the activation technique and AMS represents an important complement to online measurements, since this independent approach implies different systematic uncertainties. AMS allows measuring precisely neutron-capture cross-sections, thus elucidating current discrepancies within the *s*-process path. Besides simulating nucleosynthesis processes in the laboratory via cross-section measurements, also the direct search, e.g. for certain supernova-produced, long-lived radionuclides deposited on Earth, like ^{60}Fe, ^{182}Hf, ^{244}Pu and ^{247}Cm will give an improved insight into explosive nucleosynthesis scenarios. AMS represents a powerful and sensitive technique to search for spurious amounts of live long-lived radionuclides in terrestrial archives. Such challenging applications, where a facility has to explore its limits, are clearly beneficial also for more routine applications of AMS.

References

[1] M. Asplund, N. Grevesse, J. Sauval, in: T.G. Barnes III, F.N. Bash (Eds.), ASP Conf. Ser, vol. 336, Astron. Soc. Pac., San Francisco, 2005, p. 25.
[2] G. Wallerstein et al., Rev. Mod. Phys. 69 (1997) 995.
[3] M. Arnould, S. Goriely, Phys. Rep. 384 (2003) 1.
[4] H. Nassar, M. Paul, et al., Phys. Rev. Lett. 96 (2006) 041102.
[5] A. Arazi, T. Faestermann, J.O. Fernández Niello, K. Knie, G. Korschinek, M. Poutivtsev, E. Richter, G. Rugel, A. Wallner, Phys. Rev. C 74 (2006) 025802.
[6] R. Gallino, C. Arlandini, M. Busso, M. Lugaro, C. Travaglio, O. Straniero, A. Chieffi, M. Limongi, Astrophys. J. 497 (1998) 388.
[7] F. Käppeler, A. Mengoni, Nucl. Phys. A 777 (2006) 291.
[8] F. Käppeler, Nucl. Instrum. Meth. B 259 (2007) 663.
[9] C. Sneden et al., Astrophys. J. 591 (2003) 936.
[10] J. Ellis, B.D. Fields, D.N. Schramm, Astrophys. J. 470 (1996) 1227.
[11] G. Korschinek et al., Radiocarbon 38 (1) (1996) 68–69.
[12] B.D. Fields, K.A. Hochmuth, J. Ellis, Astrophys. J. 621 (2005) 902.
[13] K. Knie, G. Korschinek, T. Faestermann, E.A. Dorfi, G. Rugel, A. Wallner, Phys. Rev. Lett. 93 (2004) 171103.
[14] M. Paul et al., Astrophys. J. Lett. 558 (2001) L133.
[15] M. Paul et al., J. Radioanal. Nucl. Chem. 272 (2007) 243;
M. Paul et al., Nucl. Phys. A 719 (2003) C29.
[16] C. Wallner, T. Faestermann, U. Gerstmann, K. Knie, G. Korschinek, C. Lierse, G. Rugel, New Astron. Rev. 48 (2004) 145.
[17] G. Raisbeck, T. Tran, D. Lunney, C. Gaillard, S. Goriely, C. Waelbroeck, F. Yiou, Nucl. Instr. Meth. B 259 (2007) 673.
[18] C. Vockenhuber, C. Feldstein, M. Paul, N. Trubnikov, M. Bichler, R. Golser, W. Kutschera, A. Priller, P. Steier, S. Winkler, New Astron. Rev. 48 (2004) 161.
[19] C. Fitoussi et al., Phys. Rev. Lett. 101 (2008) 121101.
[20] F. Dellinger, O. Forstner, R. Golser, W. Kutschera, A. Priller, P. Steier, A. Wallner, G. Winkler, Nucl. Instr. Meth. Phys. Res. B 268 (2010) 1287.
[21] A. Wallner et al., in preparation.
[22] M. Paul, W. Henning, W. Kutschera, E.J. Stephenson, J.L. Yntema, Phys. Lett. 94B (1980) 303.
[23] H. Nassar, M. Paul, et al., Phys. Rev. Lett. 94 (2005) 092504.
[24] W. Ratynski, F. Käppeler, Phys. Rev. C 37 (1988) 595.
[25] S.K. Hui, M. Paul, D. Berkovits, E. Boaretto, S. Ghelberg, M. Haas, A. Hershkowitz, E. Navon, Nucl. Instr. Meth. B 172 (2000) 642.
[26] A. Arazi, T. Faestermann, J.O. Fernandez Niello, K. Knie, G. Korschinek, E. Richter, G. Rugel, A. Wallner, New Astron. Rev. 46 (2002) 525.
[27] B.N. Limata et al., (LUNA collaboration), private communication.
[28] M. Paul et al., Nucl. Phys. A 718 (2003) 239c.
[29] H. Nassar et al., Nucl. Phys. A 758 (2005) 411.
[30] H. Nassar et al., Annual Report 2006, Maier-Leibnitz-Laboratorium der Universität München und der Technischen Universität München (see http://www.bl.physik.uni-muenchen.de/bl_rep/jb2006/p027.pdf).
[31] H. Nassar et al., Nucl. Phys. A 746 (2004) 613c.
[32] A. Wallner et al., J. Phys. G 35 (2008) 014018.
[33] A. Wallner, M. Bichler, I. Dillmann, R. Golser, F. Käppeler, W. Kutschera, M. Paul, A. Priller, P. Steier, C. Vockenhuber, Nucl. Instr. Meth. B 259 (2007) 677.
[34] I. Dillmann, C. Domingo-Pardo, M. Heil, F. Käppeler, A. Wallner, O. Forstner, R. Golser, W. Kutschera, A. Priller, P. Steier, A. Mengoni, R. Gallino, M. Paul, C. Vockenhuber, Phys. Rev. C79 (2009) 065805.
[35] L. Coquard, F. Käppeler, I. Dillmann, A. Wallner, K. Knie, W. Kutschera, Proceedings of Science, 2006, PoS(NIC-IX)274.
[36] G. Rugel, I. Dillmann, T. Faestermann, M. Heil, F. Kaeppeler, K. Knie, G. Korschinek, W. Kutschera, M. Poutivtsev, A. Wallner, Nucl. Instr. Meth. B 259 (2007) 683;
I. Dillmann, M. Heil, F. Käppeler, T. Faestermann, G. Korschinek, K. Knie, M. Poutivtsev, G. Rugel, A. Wallner, T. Rauscher, Proceedings of Science, 2006, PoS(NIC-IX)089.
[37] I. Dillmann et al., Nucl. Instr. Meth. B 268 (2010) 1283.
[38] N. Kinoshita et al., J. Phys. G 35 (2008) 014033.
[39] M. Paul, private communication.
[40] D. Robertson, P. Collon, D. Henderson, S. Kurtz, L. Lamma, C. Schmitt, B. Shumard, J. Webb, Nucl. Instr. Meth. B 266 (2008) 3481.
[41] D. Robertson, private communication.
[42] J. Applegate, C. Hogan, Phys. Rev. D 31 (1985) 3037.
[43] T. Rauscher, J.H. Applegate, J. Cowan, F.-K. Thielemann, M. Wiescher, Astrophys. J. 429 (1994) 499.
[44] S. Merchel, M. Arnold, G. Aumaître, L. Benedetti, D.L. Bourlès, R. Braucher, V. Alfimov, S.P.H.T. Freeman, P. Steier, A. Wallner, Nucl. Instr. Meth. B 266 (2008) 4921.
[45] O. Forstner, L. Michlmayr, M. Auer, R. Golser, W. Kutschera, A. Priller, P. Steier, A. Wallner, Nucl. Instr. Meth. B 266 (2008) 2213.
[46] K. Nishiizumi, M. Imamura, M.W. Caffee, J.R. Southon, R.C. Finkel, J. McAninch, Nucl. Instr. Meth. B 258 (2007) 403.
[47] G. Korschinek, A. Bergmaier, T. Faestermann, U.C. Gerstmann, K. Knie, G. Rugel, A. Wallner, I. Dillmann, G. Dollinger, Ch. Lierse von Gostomskie, K. Kossert, M. Maitia, M. Poutivtsev, A. Remmer, Nucl. Instr. Meth. Res. B 268 (2010) 187;
Jérôme Chmeleff, Friedhelm von Blanckenburg, Karsten Kossert, Dieter Jakob, Nucl. Instr. Meth. Res. B 268 (2010) 192.
[48] M. Wiescher, J. Görres, H. Schatz, J. Phys. G 25 (1999) R133.
[49] S. Raman, M. Igashira, Y. Dozono, H. Kitazawa, J.E. Lynn, Phys. Rev. C 41 (1990) 458.
[50] T. Shima, F. Okazaki, T. Kikuchi, T. Kobayashi, T. Kii, T. Baba, Y. Nagai, M. Igashira, Nucl. Phys. A 621 (1997) 231c.
[51] H. Herndl, R. Hofinger, J. Jan, H. Oberhummer, J. Görres, M. Wiescher, F.K. Thielemann, B.A. Brown, Phys. Rev. C 60 (1999) 064614. See e.g. the "Evaluated Nuclear Data File" at the IAEA Nuclear Data Services. <http://www-nds.iaea.org/exfor/endf00.htm>..
[52] M. Lugaro et al., Astron. Astrophys. 484 (2008) L27–L30.

[53] D. Hutcheon, Nucl. Instr. Meth. A 498 (2003) 190.
[54] A. Formicola et al., Nucl. Instr. Meth. A 507 (2003).
[55] A. Di Leva et al., Nucl. Instr. Meth. A 595 (2008) 381.
[56] The n_TOF Collaboration, "CERN n_TOF Facility: Performance Report", CERN/INTC-O-011 INTC-2002-037 CERN-SL-2002-053ECT, 2002 (unpublished).
[57] S. Romano et al., J. Phys. G – Nucl. Part. Phys. 35 (2008) 14008.